Theoretical study of back-to-back avalanche photodiodes for mid- and longwave infrared applications

T. Manyk, K. Majkowycz, J. Rutkowski, P. Martyniuk

***Abstract*—**This The dual-band N^+-p-**p**-p-P^+-p-**p**-p-n^+ avalanche photodiode (APDs) structure is designed and numerically analyzed in detail. We conducted a theoretical study of APD for medium wave (MWIR) and longwave infrared (LWIR) applications. The current-voltage (*I-V*) characteristics for the bias range -6V<*U*<+15V are compared. The contribution of doping level in individual layers is shown. The following values of the ionization coefficient for electrons were used for simulation procedure $\alpha_e=3\times10^5$ m^{-1} (x_{Cd}=0.20) and $\alpha_e=3\times10^6$ m^{-1} (x_{Cd}=0.33).

I. Introduction

Infrared (IR) avalanche photodiodes (APDs) require high gain and low noise. The variable bandgap HgCdTe is a well suited material for APDs [1–3]. The paper presents the research on the APD structure with a blocking barrier (x_{Cd}=0.45) allowing to reduce the carrier concentration in the absorber region. Theoretical simulations were performed by APSYS numerical platform (by *Crosslight*) [4]. In this paper, we present the theoretical simulations of the dual-band N^+-p-**p**-p-P^+-p-**p**-p-n^+ back-to-back HgCdTe APDs. Idea of the first N-color HgCdTe detector was demonstrated in 1970s [5].

II. Avalanche Photodiode Structure and Theoretical Modeling Approach

The simulated HgCdTe APD consists of the following layers designed in the order:

CL/ML/AL/TL/BL/TL/AL/ML/CL presented in Table 1.

Table 1

The APD structure used for simulations

Region	Doping concentration (cm^{-3})	Thickness (μm)	Cd mole fraction
N^+-Contact layer (CL)	4.0×10^{17}	3	0.33
p^+-Multiplication layer (ML)	3.0×10^{14}	1	0.33
p^+-Active layer (AL)	8.0×10^{15}	5	0.33
p^+-Transient layer (TL)	1.0×10^{15}	0.1	*Grad* (0.33-0.45)
P^+-Barrier layer (BL)	1.0×10^{14}	0.3	0.45
p^+-Transient layer (TL)	5.0×10^{15}	0.1	*Grad* (0.45-0.20)
p^+-Active layer (AL)	9.0×10^{15}	7	0.2
p^+-Multiplication layer (ML)	3.0×10^{14}	1	0.2
n^+-Contact layer (CL)	1.0×10^{17}	3	0.2

The simulated detector consists of the two back-to-back photodiodes. The photodiodes operate in the MWIR and LWIR regions at T = 230 K, with cut-off wavelengths 4 μm and 9 μm, respectively. The energy band profile for unbiased APD is presented in the Fig.1. The following values of the ionization coefficient for electrons were used for simulation procedure $\alpha_e=3\times10^5$ m^{-1} (x_{Cd}=0.20) and $\alpha_e=3\times10^6$ m^{-1} (x_{Cd}=0.33) [6].

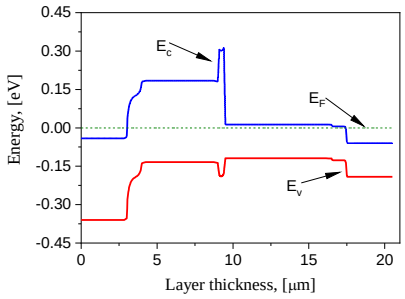

Fig. 1. Energy band profile of the simulated APD for unbiased conditions.

That APD operates in sequential mode. By switching the voltage from a positive to a negative, it is possible to detect the signal in MWIR (λ_{Peak} = 3.4 μm) and LWIR (λ_{Peak} = 6.5 μm) range. Figure 2–3 shows the band structure for both polarization within the range from U = -6V to U = +15V. The doping of individual layers influence on the *I-V* characteristics without impact ionization effect is presented in Fig. 4–5. The dark current increases versus the doping level decrease in the MWIR absorber, while a reduction in doping in the LWIR layer reduces the dark current. This effect is due to the increase in Auger recombination suppression for the low doping level in the absorber layer. The APD gain was calculated as a ratio of the dark current density with the impact ionization to the current density without the impact ionization. Figures 6–7 show the theoretically determined APD gain versus voltage for two switching modes (MWIR and LWIR photodiodes).

978-1-6654-7899-1/22/$31.00 ©2022 IEEE

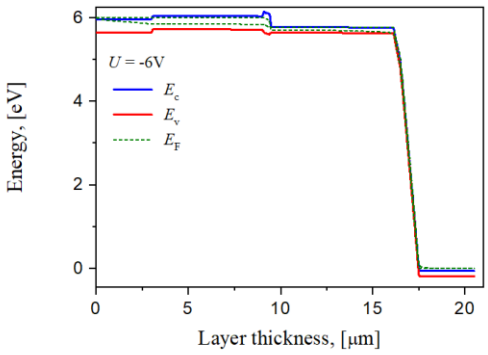

Fig. 2. Energy band profile of the simulated APD for U = -6V.

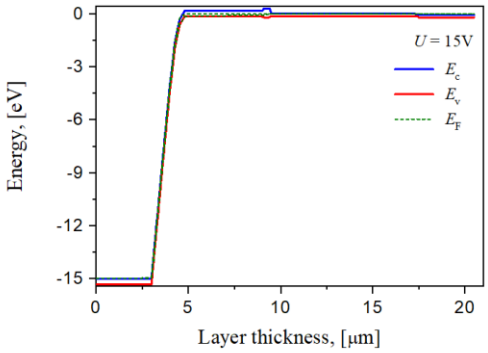

Fig. 3. Energy band profile of the simulated APD for U = +15V.

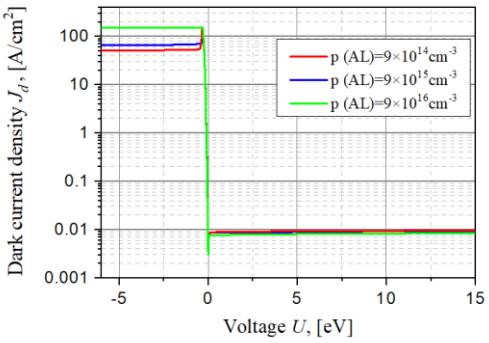

Fig. 4. Calculated *I-V* at T = 230 K for selected doping levels in the LWIR absorber layer (x_{Cd}=0.20), without impact ionization.

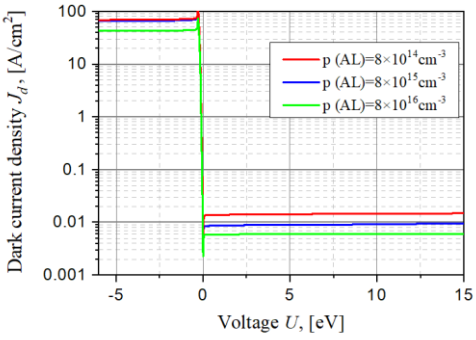

Fig. 5. Calculated *I-V* at T = 230 K for various doping levels in the MWIR absorber layer (x_{Cd}=0.33), without impact ionization.

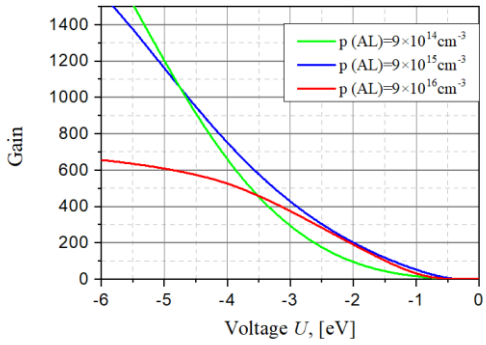

Fig. 6. The APD's gain versus voltage for selected doping levels in the LWIR absorber layer (x_{Cd}=0.20).

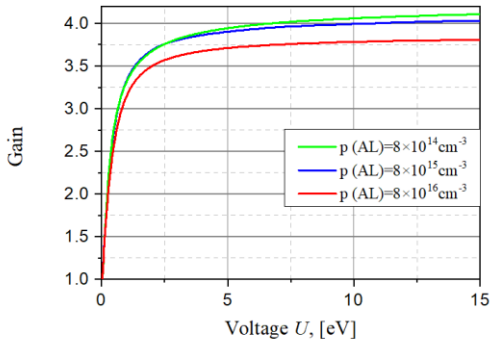

Fig. 7. The APD's gain versus voltage for selected doping levels in the MWIR absorber layer (x_{Cd}=0.33).

III. Results, Comments and Conclusions

The dual-band N^+-p-**p**-p-P^+-p-**p**-p-n^+ APD was investigated. We showed that APD gain increases for low doping in absorber layers (see Fig. 6-7). In the LWIR absorber layer the gain reaches > 1000 while in the MWIR ~ 4. This effect is probably due to the lack of Auger suppression in this absorber. The doping change in multiplication layer does not affect the current-voltage characteristics.

Acknowledgment

The National Science Centre (Poland), grant no. UMO-2019/33/B/ST7/00614.

References

[1] Beck J., Wan C., Kinch M., Robinson J. at al. "The HgCdTe electron avalanche photodiode". *Journal of Electronic Materials* 35, 6 (2006).
[2] Jiale He, Qing Li, Peng Wang, Fang Wang at al. "Design of a bandgap-engineered barrier-blocking HOT HgCdTe long-wavelength infrared avalanche photodiode". *Optics Express* 3355, 28 (2020).
[3] Rogalski A. "HgCdTe infrared detector material: history, status and outlook". *Reports on Progress in Physics* 68, 2267–2336 (2005).
[4] APSYS Macro/User's Manual ver. 2011. *Crosslight Software*, Inc. (2011).
[5] Halpert H., Musicant B. L. "N-Color (Hg,Cd)Te Photodetectors". *Applied Optics* 11, 2157–2161 (1972).
[6] Kinch M.A. "Fundamentals of Infrared Detectors Materials". SPIE Press, Bellingham, Washington, 110–112 (2007).